Soft Matter

Accepted Manuscript

ROYAL SOCIETY OF CHEMISTRY

www.rsc.org/softmatter

Polymer-Mediated Nanorod Self-Assembly Predicted by Dissipative Particle Dynamics Simulations

Shaghayegh Khani, Safa Jamali, Arman Boromand, Michael J. A. Hore and Joao Maia*

Department of Macromolecular Science and Engineering, Case Western Reserve University,
Cleveland, Ohio 44106, USA

Abstract

Self-assembly of nanoparticles in polymer matrices is an interesting and growing subject in the field of nanoscience and technology. We report herein on modelling studies of the self-assembly and phase behavior of nanorods in a homopolymer matrix, with the specific goal of evaluating the role of deterministic entropic and enthalpic factors that control the phase separation in such systems. Grafting polymer brushes from the nanorods is one approach to control/impact their self-assembly capabilities within a polymer matrix. From an energetic point of view, miscible interactions between the brush and the matrix are required for achieving a better dispersibility; however, grafting density and brush length are the two important parameters in dictating the morphology. Unlike in previous computational studies, the present Dissipative Particle Dynamics (DPD) simulation framework is able to both predict dispersion or aggregation of nanorods *and* determine the self-assembled structure, allowing for the determination of a phase diagram, which takes all of these factors into account. Three types of morphologies are predicted: dispersion, aggregation and partial aggregation. Moreover, favorable enthalpic interactions between the brush and the matrix are found to be essential for expanding the window for achieving a well-dispersed morphology. A three-dimensional phase diagram is mapped on which all the afore-mentioned parameters are taken into account. Additionally, in the case of immiscibility between brushes and the matrix, simulations predict the formation of some new and tunable structures.

Key words: Nanorods, polymer brush, nanoparticle self-assembly, controlled morphology, Dissipative Particle Dynamics

Introduction

In past decades, a plethora of experimental studies on reinforcing polymers has emerged and among the most widely used strategies for achieving enhanced properties in polymers is to prepare mixtures of them with nanoparticles (NPs) of different shapes[1-8]. Recent improvements in computational capabilities have significantly contributed to the current understanding of the NPs' phase behavior in polymer composites[9]. Spherical NPs have been incorporated into polymer matrices more commonly than other types of nanofillers, in part due to their simpler synthetic access. As such, most of the computational studies have focused on the phase behavior of this class of NPs; however, there are a wide range of NPs, which can offer superior properties that range from tubes, rods and plates with large aspect ratios to layered structures and more complex geometries. Regardless of their shape and size, spatial organization and distribution of the NPs in the matrix directly influences the macroscopic properties of nanocomposites; therefore, to maximize desired properties controlled dispersion/aggregation of these particles is required. The interactions between the NPs are perhaps the strongest barrier to achieving preferred morphologies. One of the most promising tools to overcome this barrier is NP surface modification through grafting polymer chains, which has been proven to provide control over their spatial organization in the matrix[10]. The structures formed by polymer-grafted NPs can be tuned by varying system parameters, such as volume fraction of NPs, density of grafting, degree of polymerization of the grafted polymer, miscibility between the grafted and matrix polymer. In most cases, a well-dispersed state is required for optimum mechanical and physical properties; therefore, most of the research in this area has focused on maximizing dispersion of the particles in the matrix. On the other hand, self-assembly of NPs into anisotropic superstructures can lead to formation of new functional materials[11, 12]. Thus, recently new ideas on developing techniques for controlled NP aggregation and self-assembly are being unfolded. In order to promote dispersion in a composite of this kind, grafted polymers are required to be miscible with the matrix; however, dispersibility of NPs is still affected by grafting density and brush molecular weight[10, 13]. In fact, self-assembled nanoparticle structures are formed as a result of the competition between the steric repulsions induced by the brush and the depletion interactions caused by the matrix[14]. According to the phase diagram reported by Kumar *et al.*[10], for such composites of spherical NPs, good dispersion is achieved in the limit of high grafting density due to steric stabilization. On the other hand, when NPs are only sparsely grafted, they are found to phase separate and self-assemble into a range of structures which subsequently depend on the graft molecular weight and density[15]. These findings have highlighted the important role of brush length and density in the phase behavior of polymer-grafted NPs in composite materials and have promoted interest and research in further elucidating the potential of such materials, specifically for NPs with more complex shapes.

Recently, nanorods (NRs) have attracted a lot of attention due to their shape anisotropy, as in many applications they have been found to be far more advantageous than isotropic spherical particles[7]. As mentioned earlier, having control over NRs organization, spacing and orientation is of crucial importance. For example, in applications that involve energy transfer, e.g., solar cells, partial alignment of NRs was found to be essential for significant efficiency improvement[16]. Also as shown by Wang *et al.*[17] , local ordering of NRs in aggregated structures leads to better optical properties compared to the uniformly dispersed systems. Despite the complex phase behavior observed for anisotropic particles, grafting polymer brushes on the surface of NRs is still believed to be the most effective technique for tuning the morphology[18, 19]. To enhance dispersibility, most NRs are functionalized with polymers that have identical chemistry to that of the matrix, in which case NR aggregation is an entropically driven phenomenon. Thus, the morphology can be engineered by proper selection of brush length and density[20-23]. For example, according to Frischnecht *et al.*,[22] the grafted polymer is required to be at least two times longer than the matrix for obtaining a well dispersed morphology in which the majority of the rods are isolated from each other. This indeed may put some constraints on the experiments, because either the matrix should have a low molecular weight or the brushes should be very long. Having a low molecular weight matrix can result in a reduction of mechanical properties, whereas there are some experimental limitations in using high molecular weight brushes in terms of the grafting density. According to Hore *et al.*[24] dispersion can be promoted when the brushes are energetically attracted to the matrix; however, how the miscibility parameter affects the dispersion map for the NR composites has yet to be explored in detail.

To date, most of the computational and theoretical investigations on NR aggregation are focused on finding a universal map for directing NR assembly into different structures. For example, Lin *et al*[25] reported different structures formed by aggregation of end-tethered NRs performing Dissipative Particle Dynamics (DPD) simulations. Akcora *et al*[15] in a simulation and experimental study demonstrated that polymer grafted spherical nano-particles in a polymer matrix can self-assemble into anisotropic structures depending on the brush length and density, and reported a phase diagram. Nevertheless, the specific interactions of NRs driven by their anisotropy alters this phase diagram and increases the complexity of the structures.

While previous computational studies have been successful in predicting the conditions under which nanorods will aggregate within polymer matrices, they cannot predict the self-assembled structures. For instance, while previous DFT and SCFT calculations[22, 24] provided an estimate of the interaction between nanorod pairs, they did not take into account factors such as orientational or kinetic effects. In addition, a previous DPD study by Lin *et al.*[25] was only able to produce aggregated structures by artificially driving the nanorods together. Yan et al. [26] investigated the self-assembly behavior of end-tethered NRs in a thin film of polymer blend using a multiscale computational technique. Rather than performing a systematic study they carried out DPD simulations in order to justify the empirical equations representing the interactions between the rods and the matrix in a coarse grained Cahn-Hilliard model combined with Brownian Dynamic simulations. Here, we present the results of systematic DPD simulations that are able to both reproduce the experimentally observed morphologies and predict new ones by only varying the interaction parameter between the brush and the matrix and the brush grafting density.

In this work, we comprehensively investigate the effect of enthalpic interactions combined with entropic parameters on the phase behavior of one-dimensional rigid NRs, for which we use DPD simulations. DPD is essentially a coarse-grained mesoscale method and has been recently used for simulating NRs phase behavior in polymers[25-28]. Specifically, we incorporate favorable/unfavorable enthalpic interactions into DPD simulations by adjusting the Flory-Huggins χ-parameter and present the DPD predictions, showing the effect of the enthalpic strength on the morphology in a three-dimensional phase diagram. While our simulations confirm the findings of previous experimental studies, they also predict several new structures formed by NRs in the presence of unfavorable enthalpic interactions between the brush and the matrix which have yet to be investigated in the literature.

Simulation method

Dissipative Particle Dynamics (DPD) is used in order to simulate the phase behavior of NRs in a polymer composite. DPD is a coarse-grained mesoscale simulation technique that was introduced by Hoogerbrugge and Koelman[29] in 1992 and since then has been applied to different soft matter systems[30-33] and was found to be quite promising. In DPD the Newton's equation of motion is solved for interacting particles and then is time-integrated through a modified version of the velocity-Verlet[34]. The net force acting on an individual particle is calculated as the summation over all pairwise forces inter-particle forces.

$$F_i = \sum_{i \neq j} F_{ij}^C + F_{ij}^D + F_{ij}^R,$$

The main three pairwise forces that are present in the simulations are the dissipative, random and the conservative force. The random and dissipative force together form the *NVT* ensemble and ensure the temperature conservation in the system. Random force F_{ij}^R is the heat source that generates the thermal fluctuations. Dissipative force F_{ij}^D on the other hand is the heat sink that dissipates energy from the system. The corresponding formulations are presented below.

$$F_{ij}^R = \sigma \omega^R \left(r_{ij} \right) \theta_{ij} \hat{r}_{ij} / \sqrt{dt},$$

$$F_{ij}^D = -\gamma \omega^D \left(r_{ij} \right) \left(\hat{r}_{ij} . v_{ij} \right) \hat{r}_{ij},$$

Where $r_{ij} = r_i - r_j$ is the distance between the ith and jth particles and $\hat{r}_{ij} = \frac{r_{ij}}{|r_{ij}|}$ is its unit vector. σ and γ correspond to the thermal noise and the dissipation strength respectively and θ_{ij} is the Gaussian random number with zero mean and unit variance. ω^R and ω^D are the weight functions that depend on the distance between the particles. The weight functions in the following forms are most frequently used in DPD calculations and that is what we have employed here. The fluctuation-dissipation theorem derived by Español and Warren[35] ensures the *NVT* ensemble.

$$\omega^D = \left[\omega^R\right]^2 = \begin{cases} \left(1 - \frac{r_{ij}}{r_c}\right)^2 & r_{ij} < r_c \\ 0 & r_{ij} > r_c \end{cases}$$

$$\sigma^2 = 2\gamma k_B T.$$

The conservative force F_{ij}^C is the soft repulsive potential that linearly decreases with the distance between the particles. The following form is used in our simulations.

$$F_{ij}^C = \begin{cases} a_{ij}(1 - \frac{r_{ij}}{r_c})\hat{r}_{ij} & r_{ij} < r_c \\ 0 & r_{ij} > r_c \end{cases}$$

Where a_{ij} is the interaction potential and r_c is the cutoff radius that determines the range of interaction between neighbor particles. By varying a_{ij} the immiscibility can be introduced in the system and the value of Flory-Huggins χ-parameter can be evaluated using the Groot and Warren expression[34].

In our simulations the interaction potential between the like particles is kept unchanged and $a_{ij} = 25.0$ based on the compressibility-driven expressions[34]. Number density ρ, temperature k_BT and the cutoff radius r_c are kept constant and their values are set at 3.0, 1.0 and 1.0 respectively. In a multicomponent system the interaction potential between unlike particles is defined as $a_{ij} = a_{ii} + \Delta a_{ij}$ in which Δa_{ij}, ($\frac{\chi N k_B T}{\Delta a_{ij}} = (0.306 \pm 0.003)\,\mathrm{N}$) can be related to the Flory-Huggins χ-parameter[34]. Thus a $\Delta a_{ij} = 0.0$ means that there is no enthalpic preference present between the two components while its negative value introduces favorable enthalpic interactions to the system.

According to previous studies[36, 37], and unlike the DPD simulations performed by Yan et al.[26] , in which NRs are made by organizing DPD particles in a FCC lattice, the NRs in this work are constructed by attaching rigid DPD particles together (Figure 1), which results in less expensive computations. The center-to-center distance between two consecutive particles along the nanorod is fixed at a small value which is $0.2r_c$. Thus the density of particles on the nanorods is increased (~6.5) which consequently prevents overlapping and unphysical crossings. The whole rod is considered as one rigid body and the equations of motion are solved with regards to the rigid body dynamics. Polymer chains are modeled using a spring potential which acts between the consecutive segments forming a bond.

$$F^S = k_s(r_{ij} - r_{eq})\,\hat{\mathrm{r}}_{ij}$$

Where k_s is the spring constant set at 20 and r_{eq} is the equilibrium bond length (r_{eq} = 0.85). Using the same potential polymer brushes are covalently attached to the NRs at fixed grafting sites, however, shorter bonds considered where the chains are connected to the rods (r_{eq}

= 0.2). It should be noted that the grafting sites are always fixed on the NRs but the grafted chains are free to move around the rods' centerline. Although the dispersibility of the nanoparticles can be affected when the grafting sites are allowed move on the surface of the particles[38], this matter is out of the scope of the current study and is in fact the subject of an ongoing work by this group.

Rod length is set at 8.8r$_c$ and concentration of polymer grafted NRs in the calculation box $\phi = (n_R + n_b)/n_{total}$ (n_R and n_b are the number of rod and brush segments respectively) is kept constant (~0.1). Matrix polymers are made of 15 DPD beads which remains unchanged throughout this work. Calculations were carried in 40*40*40 and 65*65*65 boxes in order to ensure that the cell size does not affect the results. All the simulations were ran for $8*10^5$ time steps (with $\Delta t=0.01$) and the systems are considered to be equilibrated when they are stable for over a quarter of the calculation time. Number of grafted chains N_b, Length of the brush L_b and the miscibility between the brush and the matrix Δa_{bm} are the parameters that will be varied in this study.

Results and discussion

We base our discussion on previous experimental reports in which NRs were grafted with brushes of the same chemistry as the matrix. Therefore, we start from the entropic segregation of NRs. In this case, no enthalpic interaction is present between the brushes and the matrix polymer. As demonstrated in Figure 1, the strength of the interaction potential between the system components a_{ij} can be related to the Flory-Huggins χ-parameter[34]. So here $\Delta a_{bm} = 0$ where subscript b and m represent the brush and the matrix respectively. We study the effect of brush length and grafting density on the phase behavior of NRs in a homopolymer. As schematically shown in Figure 1, the rigid one-dimensional NRs are selectively grafted with polymers using spring potentials. The details of the simulation technique were described in the previous section.

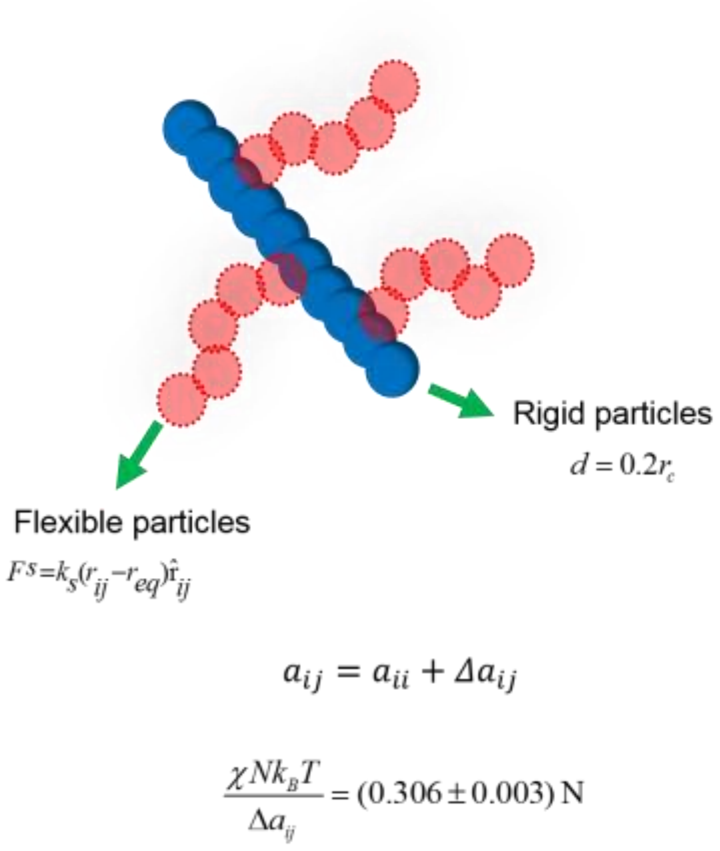

Figure 1. Schematic representation of the simulated polymer grafted NRs

a) Entropic segregation of NRs:

Our discussion begins with the phase behavior of bare NRs in a polymer matrix. As shown in Figure 2, bare NRs tend to aggregate and form structures with local ordering in which the rods are aligned side-by-side. The radial distribution function *g(r)* for the center of mass of the rods is shown in Figure 2A, which confirms the ordering of the rods in local crystalline structures. The first peak at $r = 0.95r_c$ stands for the parallel alignment of the rods and the periodic peaks at $2r$, $3r$, $4r$,… show the crystalline ordering of the rods in the aggregates. However, the order disappears above a certain point, r=9.3, and the $g(r)$ value becomes less than unity, which shows the discontinuity of the structure in the calculation box. According to previous theories[39, 40] aggregation of the NRs is attributed to the depletion that results in a fully entropic attraction between them with their side-by-side alignment being due to the excluded volume effects. Grafting polymers on the NRs will result in a competition between the steric repulsions and depletion attraction. The interplay between these two entropic factors determines the final morphology of the system. Thus, density of grafting and degree of polymerization of the brush are the two most important deterministic factors that influence the phase behavior of the NRs. So as will be discussed in the following, we have monitored the morphology changes with respect to the grafting density N_b and brush length L_b. In our observations, the degree of polymerization of the matrix ($L_m=15$) and the concentration of grafted NRs are kept constant (~ 0.1).

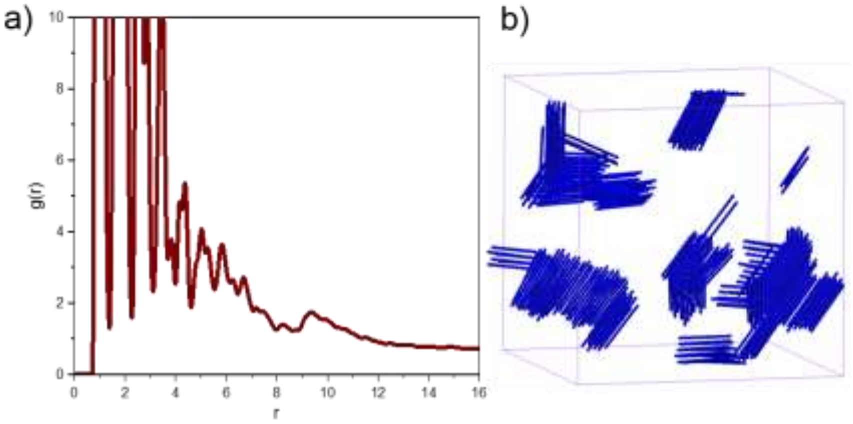

Figure 2.a) Center of mass radial distribution function and b) Snap shot shows the parallel alignment of bare NRs in aggregates.

Firstly, we measured the radial distribution function *g(r)* for the center of mass of the rods at different degrees of grafting (Figure 3A-D). As shown in Figure 3A, when only one chain is grafted in the mid-point of the rods a very similar structure to what was observed for bare NRs is obtained. Furthermore, this structure remains almost independent from the degree of polymerization of the brush and no significant change is observed in *g(r)* upon increasing the brush length, suggesting that at these low grafting densities, depletion forces remain dominant in defining the microstructure and assembly of the NRs. However, for higher degrees of grafting (Figure 3B-D), some structural changes are observed upon increasing the length of the brush. For example, as shown in Figure 3B when 5 chains are homogeneously grafted on the NRs increasing the length of the brush results in disappearance of the discontinuous large aggregates with local crystalline ordering and appearance of smaller aggregates that are distributed in the calculation cell in which the NRs are aligned side-by-side. In densely grafted NRs (Figure 3D $N_b=22$), some local alignment of the rods is still present for short chains; however, increasing the brush length results in a uniform dispersion of the rods and as is evident from the *g(r)* data, the degree of polymerization of the brush can be used in order to control the spacing between the NRs. Some of the corresponding snapshots are presented in Figure 3E, which shows the structural changes depending on the grafting density and the length of the brush.

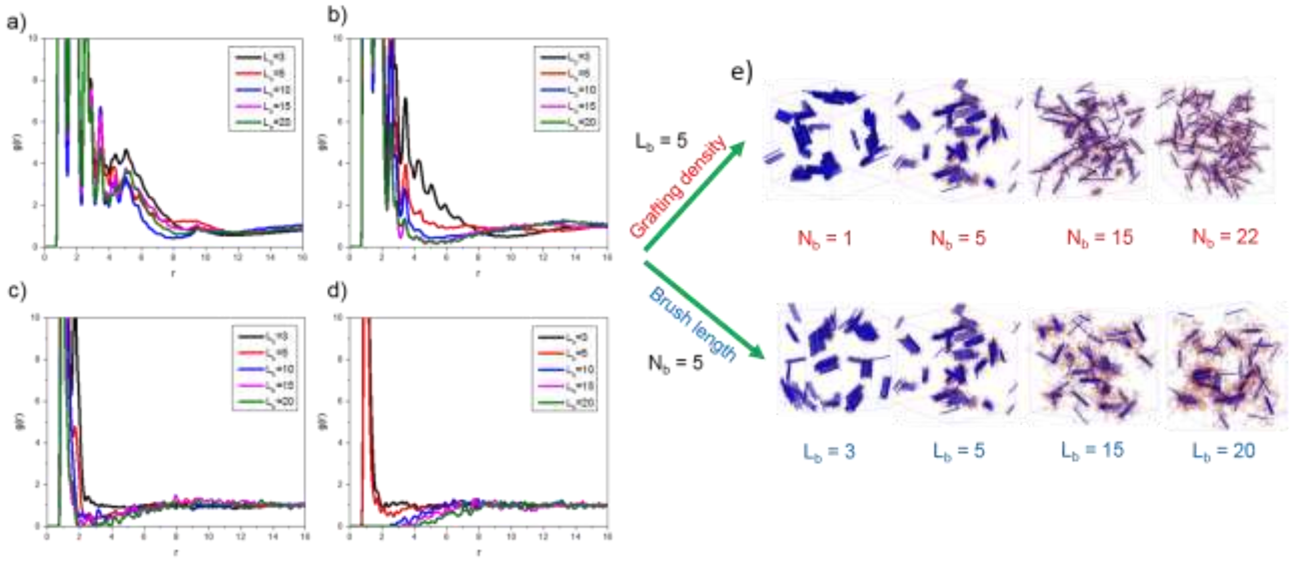

Figure 3.Center of mass radial distribution function for a) N_b=1, b) N_b=5, c) N_b=15 and d) N_b=22. L_b and N_b stand for the brush length and grafting density respectively. e) Snapshots show the effect of brush length and density on the structure of NRs.

In order to measure the dispersibility of NRs in the polymer matrix, we developed a new algorithm. In this approach, two rods are considered to be in contact when the closest distance between them is shorter than the first minima in the *g(r)* graph and larger than the first maxima peak for the bare NRs which in our case is defined to be 1.1r_c; thus, using this definition the average number of contact points on each rod is counted for each simulated system. As shown in Figure 4A-E, the results are presented as the probability of finding NRs with a certain number of contacts. The probability of finding NRs with zero number of contacts can provide a good measure of the NRs dispersion in the system. As shown in Figure 4A this value is negligible, when only one chain is grafted onto the NRs and increasing the chain length does not influence the dispersibility of NRs. This probability increases with increasing grafting density and degree of polymerization of the brush, meaning that dispersion is promoted in the system (Figure 4B-E).

As shown in Figure 4E, when NRs are densely grafted with long chains, more than 80% of the NRs are found to be individually dispersed in the system. The effect of grafting density and brush length on the probability of finding individual NRs is summarized in Figure 4F. With this information, we defined a criteria for dispersibility in which three types of morphologies are predicted: a) dispersion when more than 80% of the NRs have no contacts (P(0) ≥ 80%); b) aggregation in which P(0)<40%; and c) partial aggregation in which a small portion of NRs are aligned side-by-side and located in small aggregates. The small aggregates in the latter morphology are observed to be end-to-end connected and form a network structure that percolates in the calculation box. This structure is very similar to experimental findings and Monte Carlo simulations of Jiang *et al.*[12] for P2VP-AuNRs in P2VP films; however, their observations were limited to two dimensional specimens while what we predict here is fully three-dimensional.

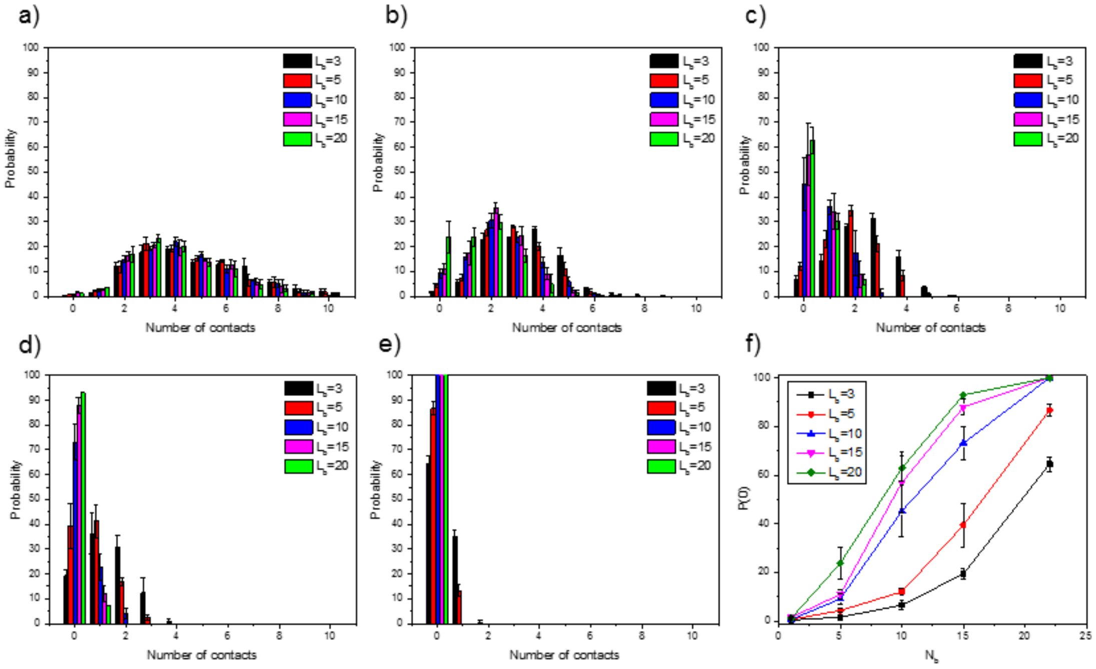

Figure 4. Distribution of the number of contacts for a) N_b=1, b) N_b=5, c) N_b=10, d) N_b=15, e) N_b=22 and f) P(0) as a function of N_b for different L_b.

Based on this dispersibility criteria, a phase diagram can be plotted with respect to the brush length L_b and grafting density N_b. Figure 5 represents the phase diagram in the absence of enthalpic interactions. Also shown in the figure are snap shots for the three different morphologies. According to the phase diagram, a well-dispersed morphology is obtained only over a very narrow range when long chains are densely grafted on the NRs.

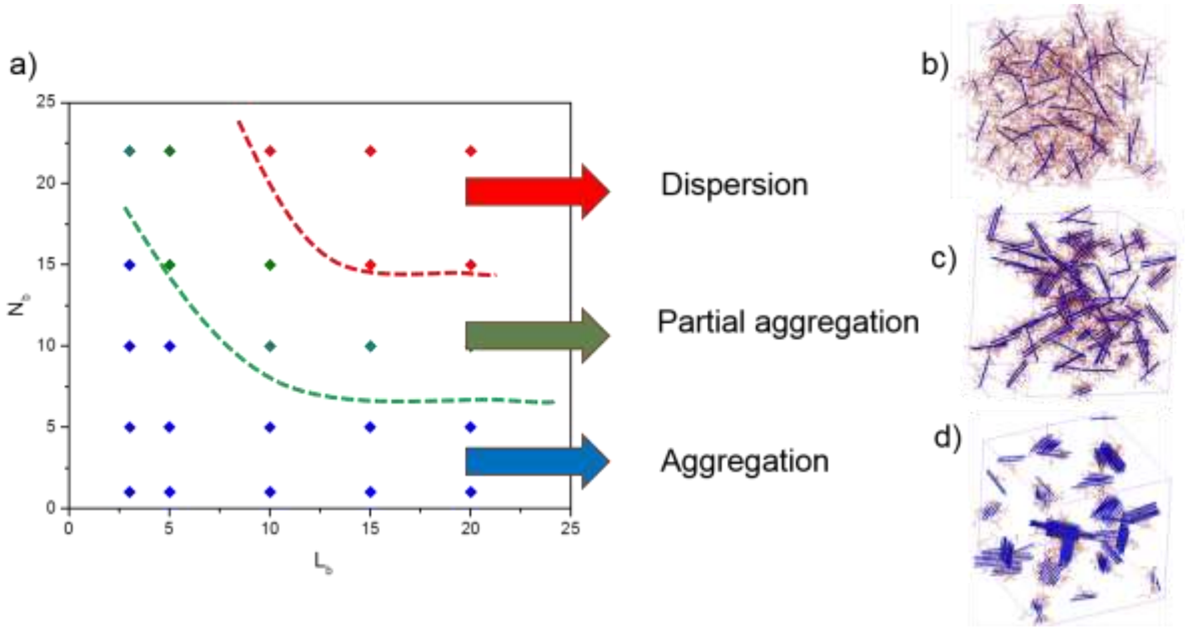

Figure 5. Phase diagram for polymer grafted NR composites with no enthalpic preference (Δa_{bm}=0). Snap shots show: a) dispersion, b) partial aggregation and c) aggregation.

These results are in qualitative agreement with the experimental observations of Wang et al[17] who studied the phase behavior of polymer (PS) grafted AuNRs in a homopolymer matrix of PS. They showed that dispersion/aggregation of NRs can be controlled by adjusting the brush molecular weight; however they did not include the effect of grafting density. Also, side-by-side alignment of rods is dominant in aggregated structures of high aspect ratio NRs, which is attributed to the depletion attractions.

So far the enthalpic interactions between the brush and the matrix have been neglected, so we next examined the microstructural consequences of energetic attraction between the polymer matrix and the grafted brushes on the NRs.

b) Favorable enthalpic interactions:

Favorable enthalpic interactions are known to be effective in promoting dispersion in a system[7]; however, this matter requires more detailed investigations and in the following we will discuss the effect of enthalpic interactions on the phase diagram defined above. Similar to the previous section we start from the radial distribution function of the center of mass of the rods (Figure 6A-D). Nevertheless, it should be noted that the nature of the polymer-brush interactions in these systems is highly attractive promoting favorable enthalpic interactions ($\Delta a_{bm} = -9.5$). As shown in Figure 6A, when the NRs are barely grafted the enthalpic interactions are not strong enough to prevent the rods from aggregating; therefore, the morphology remains unchanged and independent from the length of the brush. However, increasing the brush length results in stronger structural changes in the system compared to the equivalent case without enthalpic interactions. It is evident from the graphs that a uniform dispersion of NRs is accessible over a broader range of brush length and density compared to the previous (entropic only) case.

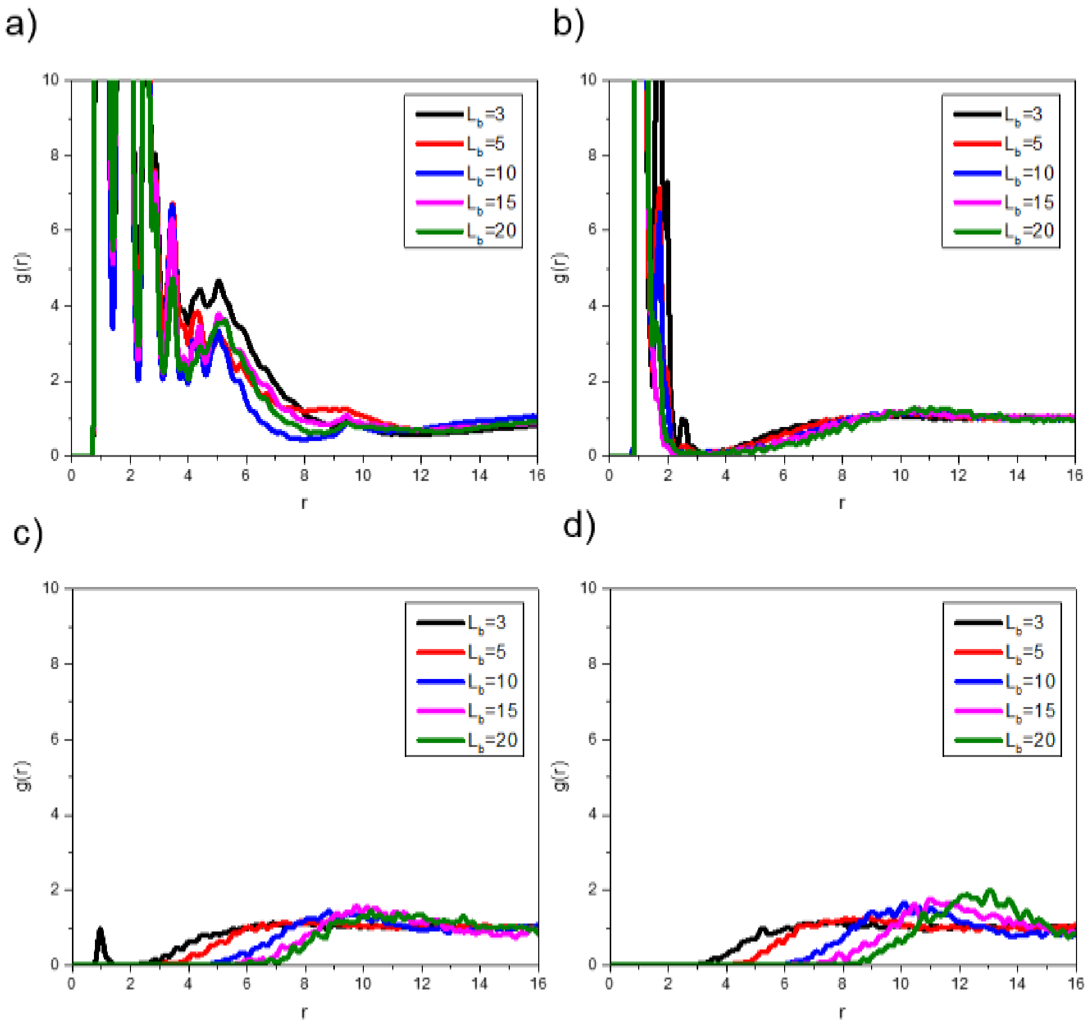

Figure 6.Radial distribution function for a) N_b=1, b) N_b=5, c) N_b=15 and d)N_b=22**.**

Additionally, the previously described algorithm to calculate the number of contacts is used to measure the dispersion of NRs in the same systems but with favorable enthalpic interactions turned on. In Figure 7A-D, similar to the approach explained in previous section, P(0) is plotted as a function of grafting density N_b, where each graph represents the results for a certain length of the brush (L_b=1 to 20) and the value of Flory-Huggins χ-parameter. The latter is achieved by varying the brush-matrix repulsion parameter (Δa_{bm}) from 0 (theta condition) to -12 (highly favorable) in order to investigate the effect of enthalpic interactions on dispersion of

NRs. As is evident from the graphs, for low degrees of grafting no significant change is observed in the value of P(0), which can be attributed to the lack of sufficient enthalpic strength to result in dispersion. Nevertheless, the probability of finding individual NRs is an increasing function of grafting density. This behavior is more obvious when the brushes are enthalpically favored by the matrix. In one graph (*e.g.* Figure 7A), as the attraction becomes stronger, a larger value is measured for P(0), which means that dispersion is occurring at relatively lower degrees of grafting until a point where the curves merge and the results become independent from the strength of the enthalpic interactions. As the length of the brush increases the curves start to merge at relatively weaker attractions. This is due to the combination of entropic and enthalpic forces that both fight against the NRs aggregation and facilitate dispersion in the system. In other words, the effect of enthalpy is more pronounced and more distinguishable when shorter brushes are grated on the NRs.

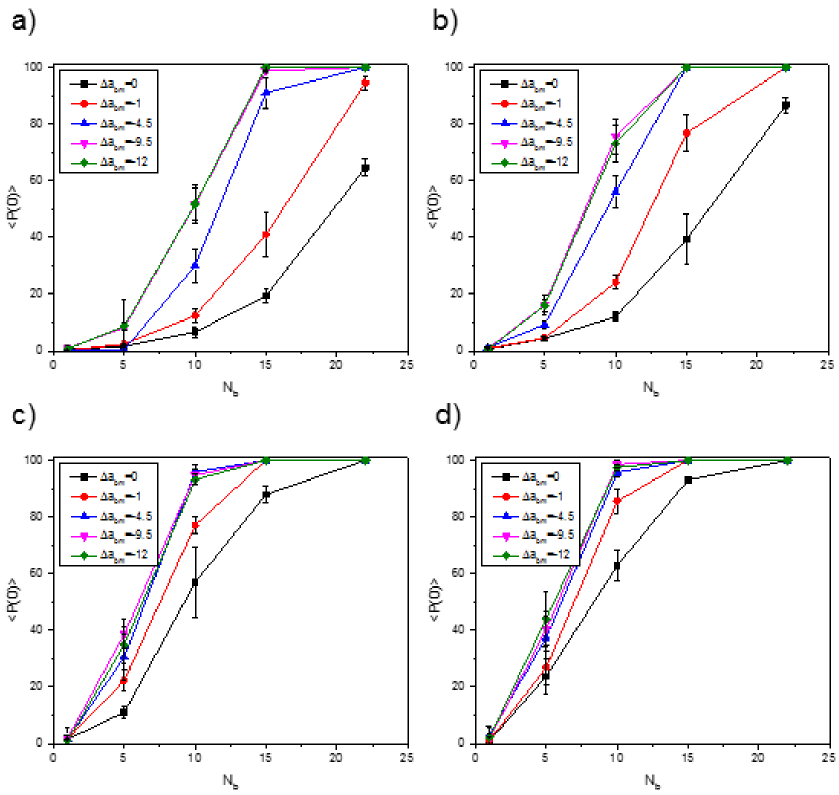

Figure 7.Effect of enthalpic interactions on the probability of finding isolated NRs P(0) as a function of grafting density for: a)L_b=3, b) L_b=5, c) L_b=15 and d) L_b=20. Δa_{bm} is equivalent to the Flory-Huggins χ-parameter.

As confirmed by P(0) measurements as well as the results for radial distribution function (Figures 6 and 7), dispersion is considerably improved *via* switching on favorable interactions between the brush and the matrix. In fact, incorporating attractive interactions in the system may result in phase transitions. For example, as shown is Figure 7E, at N_b=5 a transition from an aggregated structure to the limit of partial aggregation is observed upon introducing favorable enthalpic interactions. The calculated mean squared radius of gyration of the brush for the corresponding system with respect to the enthalpic strength (Δa_{bm}) is represented in Figure 8. Evidently, the changes in the morphology (shown in Figure 8B and C) in response to the attractive interactions can be correlated to the brush expansion. In other words, the brushes tend to increase their contact when they are energetically attracted to matrix, which consequently will obstruct NR aggregation.

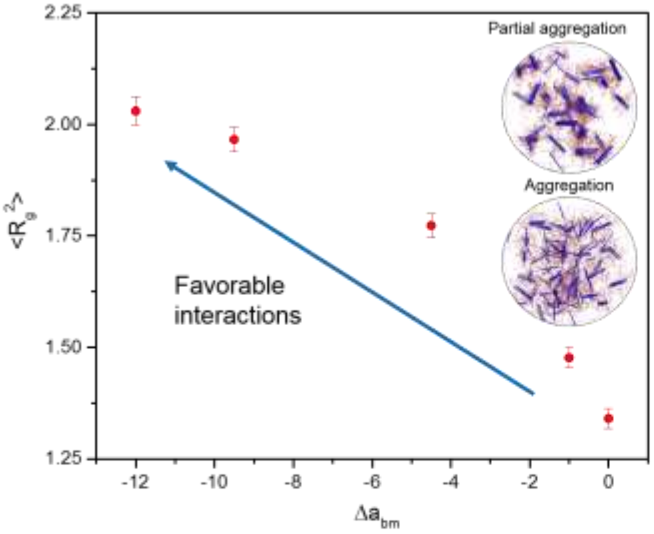

Figure 8.a) Mean square radius of gyration for (N_b=5 and L_b=15) as a function of brush-matrix interaction parameter (Δa_{bm}), Inserted snapshots show the representative aggregation and partial aggregation of the NRs.

With the detailed morphology and microstructural information at hand, one can provide a phase diagram considering the already defined dispersibility criteria for an enthalpically mixing-favored mixture. Thus Figure 9 shows a phase diagram similar to the one in the previous section that now includes highly attractive brush-matrix interactions (Δa_{bm}= -9.5). As compared to the diagram shown in Figure 5 where only a narrow window was predicted for dispersion, it is evident that the contribution of enthalpic interactions significantly broadens the dispersion area.

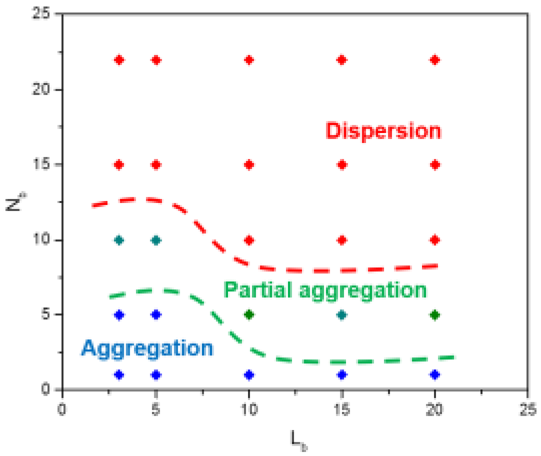

Figure 9. Phase diagram for Δa_{bm}= -9.5; dashed lines are only to guide the eye.

These results allow us to plot, for the first time, a three-dimensional phase diagram that takes into account the contribution of enthalpy as well as the brush length and grafting density (Figure 10). Clearly, the phase diagram shows that long brushes are required to be grafted on NRs at a high desnity of grafting in order to achieve a well-dispersed morphology for systems without favorable enthalpy. As the strength of attraction between the brush and the matrix increases and moves in the phase diagram to more negative values of Δa_{bm} the dispersion window becomes broader. However, in the limit of low grafting densities, NRs always aggregate and brush length and enthalpic interaction seem to be ineffective. On the other hand, favorable enthalpy makes dispersion accessible even when relatively short brushes are grafted on the NRs, provided the degree of grafting is kept high enough. Partial aggregation is predicted for NRs in between the dispersion and aggregation regimes where small aggregates of NRs are distributed throughout the calculation box and end-to-end connected which is due to the relatively high aspect ratio of the rods.

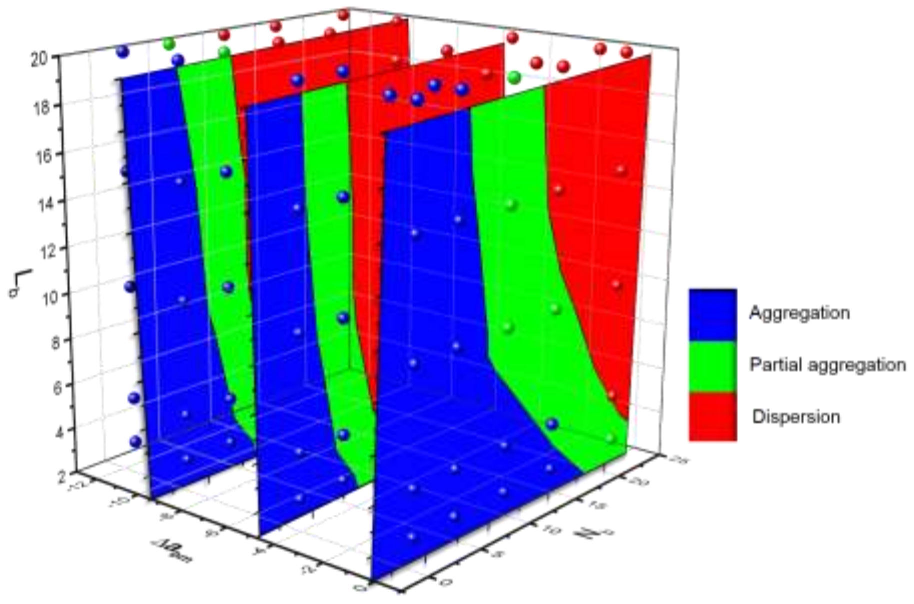

Figure 10. Three dimensional phase diagram. Dispersion, partial aggregation and aggregation are shown with red, green and blue balls respectively and the contour maps for three different planes are added to the 3D diagram to guide the eyes.

Remarkably, at a very low degree of grafting (N_b=1 only one chain is grafted on the middle point of the NRs) when the brushes are strongly attracted to the matrix (in the aggregation regime), simulation predicts the formation of a new structure formed by the NRs that to date has not been reported experimentally. In this structure which appears to be formed in a two-step process, firstly the NRs aggregate in bundles and then the bundles become end-to-end connected and form a heterogeneous network. Hypothetically, when the NRs come close to each other, due to the excluded volume effect and strong attractions between the brush and the matrix, the grafted chains are expelled from the volume within the NRs and the rods align parallel to each other. As a result, polymer brushes form an outer shell that covers the bundle of NRs in the center region until a point where the area around the aggregate becomes inaccessible for the approaching rod. Consequently, the aggregation process continues through end-to-end connection of the bundles. More interestingly, this morphology is observed as long as the grafted chains are smaller than the matrix polymer, and the network breaks down into smaller aggregates as soon as the radius of gyration of the brush exceeds that of the matrix (see Figure 11). Although quantitatively no considerable difference is observed for the structural measurements (namely the radial distribution function) this morphology is clearly observed visually in the snap shots. We speculate that the enthalpic attraction between the brush and the matrix plays a major role in formation of this structure and this may be the reason that this morphology is not predicted for entropically segregating systems.

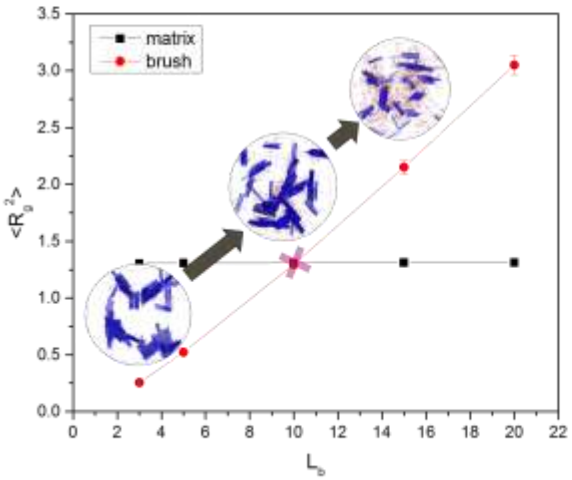

Figure11. Mean radius of gyration of polymer matrix and the brush at different interaction parameters associated with corresponding morphology snapshots as inserts for the N_b=1. Particle networks breaks into small aggregates when the size of the brush becomes larger than the matrix.

So far we have focused on miscible systems and it was shown that the combination of brush length and grafting density can be used to engineer the organization of high aspect ratio rigid NRs in the same polymer matrix. In the following section, we will present some of our model predictions for the conditions when the brushes dislike the polymer matrix (promoting demixing). To the best of our knowledge, despite their practical relevance such systems have not been explored neither experimentally nor theoretically.

c) Unfavorable enthalpic interactions:

In this part, we report some of our predictions for the phase behavior of polymer composites with NRs that are grafted with brushes being repelled by the matrix. Obviously, in this situation NRs' aggregation is inevitable from both the entropic and the enthalpic points of view, so such systems are very difficult to be studied experimentally. Using computer simulations, however, we show that in these types of composites, unfavorable interactions between the brush and matrix can result in formation of some novel and tunable structures of NRs. The observed morphology is a factor of the brush content and the degree of immiscibility between the grafted chains and the matrix. We start the discussion by looking at densely grafted NRs. In this case, due to the large number of unfavorable interactions in the system, the brushes tend to minimize the interface with the matrix. Thus, as shown in Figure 12 A and B, the major observed morphology is a spherical droplet whose size depends on the length of the brush. Three aggregates are present in the snapshot shown in Figure 12 A, while there are only two (larger) aggregates in Figure 12 B. No evidence of ripening of the aggregates are observed within the timescales achieved by the simulations.

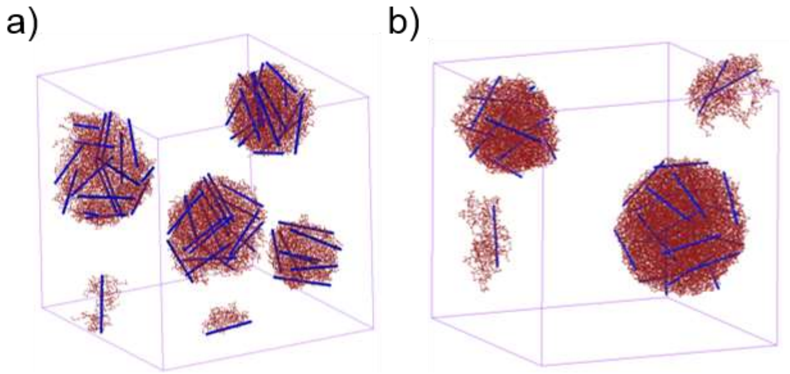

Figure 12. Observed spherical morphology for densely grafted NRs (N_b=22) with strong repulsions between the brush and the matrix (Δa_{bm}=9.5) for a) L_b=10 and b) L_b=20.

Furthermore, in the same system shown in Figure 12 A, as the degree of grafting is decreased to its minimum extreme where only one chain is grafted on the NRs, the morphology will change into a new structure for which we use the term “triangular micelle” which is represented in Figure 13 A. As shown in Figure 13 B, these micelles will transform into a “sheet-like” morphology when the degree of repulsion between the brushes and the polymers is reduced (to Δa_{bm}=4.5).

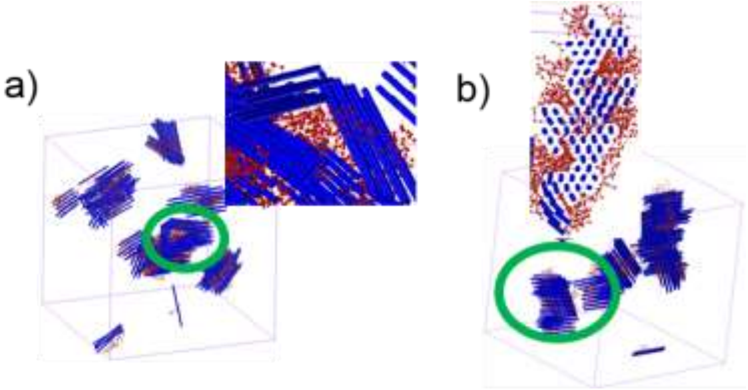

Figure 13. Morphology of sparsely grafted NRs (N_b=10) with brushes of L_b=10 for a) Δa_{bm}=9.5 and b) Δa_{bm}=4.5.

It was shown that the number of brushes on NRs as well as the interaction potential plays a major role in defining the final morphology. Keeping the composition of the brush and the interaction potential constant and mildly repulsive (Δa_{bm}=4.5), in the following we briefly explore the effect of entropic factors (brush length and grafting density) on self-organization of NRs and the obtained structures. In the snapshot shown in Figure 14A, 5 chains consisting of 3 DPD particles are grafted on each NR while the NRs in Figure 14B are only grafted with one chain of a length of 15. The brush content and the repulsion value remains the same in both figures; however, the simulations predict different type of morphologies. Similarly, in Figures 15C and D, only by switching between the degree of grafting and the length of the brush can result in a transformation from a chiral structure to spherical aggregates.

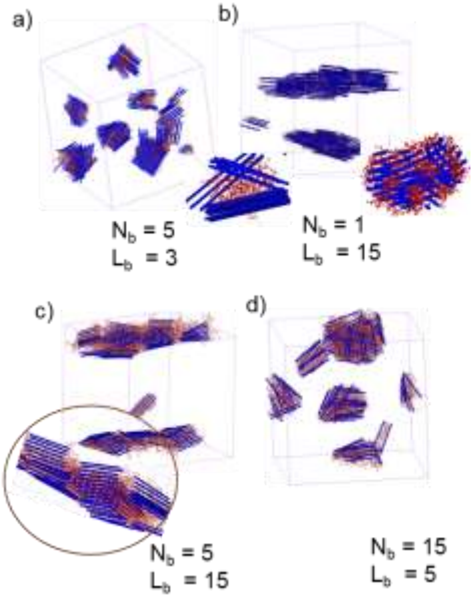

Figure 14.Effect of brush length and density on the morphology of the systems while keeping the repulsion strength and brush content constant

Conclusions

In this work, a comprehensive and detailed study of the governing mechanisms and effective factors in defining the final morphology and self-assembly of NRs in polymeric matrices was presented. Namely, by using a coarse-grained mesoscale model (DPD) the role of the deterministic factors in the phase behavior of polymer NR composites was investigated. Dispersing NRs is found to be more complicated than spherical nanoparticles which is due to their higher aspect ratio. High aspect ratio NRs tend to aggregate even in a miscible matrix and this is known to be purely entropic and a result of depletion attractions. A well-known strategy for dispersing NRs in the matrix is to graft them with a polymer chain that is chemically identical to the matrix. In this case, the aggregation are entropically favored and dependent on the grafting density and the length of the brush. We presented, and validated against experimental data available in the literature, a phase diagram with respect to these two parameters and three different regions were predicted. Good dispersion is achieved only when long enough chains are grafted on the NRs at a high degree of grafting. In the limit of low grafting density the steric repulsions from the brushes is never enough for preventing the aggregation. A region of partial aggregation is predicted between the dispersion and aggregation in which small aggregates of side-by-side NRs are distributed in the matrix and end-to-end connected. We then investigated the effect of enthalpic interactions on NR dispersion and aggregation and for the first time a three dimensional phase diagram was mapped including all the mentioned parameters. We found that the strong attractive interaction between the matrix and the brushes significantly broadens the window for dispersion. However, this parameter remains ineffective for low grafting densities. Generally, in a NR composite where enthalpic interactions are excluded, a uniformly dispersed state is available only when the brushes are longer than the matrix and this can impose constraints on the experiments. On the other hand, including attractive interactions between the brush and the matrix makes dispersion accessible even when the brushes are short; however, a minimum degree of grafting is required. We have also predicted the arrangement of NRs into a novel structure that resembles a heterogeneous network formed by parallel alignment of the rods. The exact mechanism behind the formation of this morphology is not fully clear and is currently the focus of further research. Additionally, we have shown that unfavorable enthalpic interactions can lead to formation of more complicated structures that can be tuned by adjusting the system parameters. It is important to note that all these aggregates are dynamic in a sence that they move in the calculation box, whereas no evidence of coarsening was observed within the simulation timescales and the aggregates merely exchange individual NRs. Some of these structures can be manipulated for fabrication of new nano devices; however, despite its novelty and potential importance, this type of composites have not attracted enough attention due to experimental/synthetic complications. The results predicted by mesoscale simulations shed some light into this matter and can be used as a tool for directing new experiments.

Acknowledgments

The authors would like to acknowledge the financial support from CLiPS (NSF STC grant 0423914). We also thank the help from High Performance Clusters (HPC) at CWRU that provided us with computing power. Most importantly, we are very thankful to Stuart Rowan for the constructive discussions and comments that helped us to improve the manuscript to this stage.

References

1. V. Canpean, A. M. Gabudean and S. Astilean, *Colloids and Surfaces A: Physicochemical and Engineering Aspects*, 2013, **433**, 9-13.

2. S. K. Kumar and R. Krishnamoorti, *Annual Review of Chemical and Biomolecular Engineering*, 2010, **1**, 37-58.
3. R. C. Ferrier, H.-S. Lee, M. J. A. Hore, M. Caporizzo, D. M. Eckmann and R. J. Composto, *Langmuir*, 2014, **30**, 1906-1914.
4. S. Jamali, M. C. Paiva and J. A. Covas, *Polymer Testing*, 2013, **32**, 701-707.
5. A. Bansal, H. Yang, C. Li, K. Cho, B. C. Benicewicz, S. K. Kumar and L. S. Schadler, *Nat Mater*, 2005, **4**, 693-698.
6. R. Inoubli, S. Dagréou, A. Lapp, L. Billon and J. Peyrelasse, *Langmuir*, 2006, **22**, 6683-6689.
7. M. J. A. Hore and R. J. Composto, *Macromolecules*, 2013, **47**, 875-887.
8. K. I. Winey and R. A. Vaia, *MRS Bulletin*, 2007, **32**, 314-322.
9. Q. H. Zeng, A. B. Yu and G. Q. Lu, *Progress in Polymer Science*, 2008, **33**, 191-269.
10. S. K. Kumar, N. Jouault, B. Benicewicz and T. Neely, *Macromolecules*, 2013, **46**, 3199-3214.
11. J. F. Moll, P. Akcora, A. Rungta, S. Gong, R. H. Colby, B. C. Benicewicz and S. K. Kumar, *Macromolecules*, 2011, **44**, 7473-7477.
12. G. Jiang, M. J. A. Hore, S. Gam and R. J. Composto, *ACS Nano*, 2012, **6**, 1578-1588.
13. G. D. Smith and D. Bedrov, *Langmuir*, 2009, **25**, 11239-11243.
14. A. Jayaraman and K. S. Schweizer, *Macromolecules*, 2009, **42**, 8423-8434.
15. P. Akcora, H. Liu, S. K. Kumar, J. Moll, Y. Li, B. C. Benicewicz, L. S. Schadler, D. Acehan, A. Z. Panagiotopoulos, V. Pryamitsyn, V. Ganesan, J. Ilavsky, P. Thiyagarajan, R. H. Colby and J. F. Douglas, *Nat Mater*, 2009, **8**, 354-359.
16. W. U. Huynh, J. J. Dittmer and A. P. Alivisatos, *Science*, 2002, **29**, 2425-2427
17. D. Wang, M. J. A. Hore, X. Ye, C. Zheng, C. B. Murray and R. J. Composto, *Soft Matter*, 2014, **10**, 3404-3413.
18. D. Fava, Z. Nie, M. A. Winnik and E. Kumacheva, *Advanced Materials*, 2008, **20**, 4318-4322.
19. S. Park, J.-H. Lim, S.-W. Chung and C. A. Mirkin, *Science*, 2004, **303**, 348-351.
20. P. G. Ferreira, A. Ajdari and L. Leibler, *Macromolecules*, 1998, **31**, 3994-4003.
21. M. W. Matsen and J. M. Gardiner, *The Journal of Chemical Physics*, 2001, **115**, 2794-2804.
22. A. L. Frischknecht, M. J. A. Hore, J. Ford and R. J. Composto, *Macromolecules*, 2013, **46**, 2856-2869.
23. M. J. A. Hore, A. L. Frischknecht and R. J. Composto, *ACS Macro Letters*, 2011, **1**, 115-121.
24. M. J. A. Hore and R. J. Composto, *Macromolecules*, 2012, **45**, 6078-6086.
25. Y.-L. Lin, C.-S. Chiou, S. K. Kumar, J.-J. Lin, Y.-J. Sheng and H.-K. Tsao, *The Journal of Physical Chemistry C*, 2011, **115**, 5566-5577.
26. L.-T. Yan, E. Maresov, G. A. Buxton and A. C. Balazs, *Soft Matter*, 2011, **7**, 595-607.
27. Z. Yang, L. Xin-Ping and Z. Qing-Xuan, *Polymer*, 2011, **52**, 6110-6116.
28. L. He, L. Zhang, Y. Ye and H. Liang, *The Journal of Physical Chemistry B*, 2010, **114**, 7189-7200.
29. P. J. Hoogerbrugge and J. M. V. A. Koelman, *EPL (Europhysics Letters)*, 1992, **19**, 155.
30. S. Jamali, M. Yamanoi and J. Maia, *Soft Matter*, 2013, **9**, 1506-1515.
31. D. Irfachsyad, D. Tildesley and P. Malfreyt, *Physical Chemistry Chemical Physics*, 2002, **4**, 3008-3015.
32. A. Alexeev, W. E. Uspal and A. C. Balazs, *ACS Nano*, 2008, **2**, 1117-1122.
33. S. Khani, M. Yamanoi and J. Maia, *The Journal of Chemical Physics*, 2013, **138**, -.
34. R. D. Groot and P. B. Warren, *The Journal of Chemical Physics*, 1997, **107**, 4423-4435.
35. P. Español and P. Warren, *EPL (Europhysics Letters)*, 1995, **30**, 191.
36. L. He, Z. Pan, L. Zhang and H. Liang, *Soft Matter*, 2011, **7**, 1147-1160.
37. M. J. A. Hore and M. Laradji, *The Journal of Chemical Physics*, 2008, **128**, 054901.
38. H. Chao, B. A. Hagberg and R. A. Riggleman, *Soft Matter*, 2014, **10**, 8083-8094.
39. L. Onsager, *Annals of the New York Academy of Sciences*, 1949, **51**, 627-659.

40. M. Surve, V. Pryamitsyn and V. Ganesan, *Macromolecules*, 2006, **40**, 344-354.